Calibrated Measurements and Nonlinearity Compensation of Narrowband Amplifiers

Tom Van den Broeck

Abstract—**A vectorial nonlinear-network analyzer (VNNA) is absolutely calibrated in amplitude and phase for narrowband measurements of nonlinearities. Calibration is performed with a reference generator, characterized with a calibrated sampling oscilloscope. The reference signal, consisting of an upconverted baseband signal, is optimized for high signal-to-noise ratio measurements. Using the calibrated VNNA, narrowband amplifiers can be measured, enabling compensation of intermodulation and crossmodulation.**

I. Introduction

IN THIS PAPER the vectorial nonlinear-network analyzer concept [1] is extended for measuring narrowband devices. This is very important for testing and designing narrowband communication systems. Several mathematical tools exist for describing and analyzing nonlinear components [2], [3]. However, measuring these systems is a difficult problem. In case a parametric model of the DUT is available, Maas [4], [5] proposed a method using a spectrum analyzer setup and DC measurements. For nonparametric models, however, phase measurements are required to complement the amplitude information. Lott [6] presented a frequency domain approach based upon a conventional network analyzer. This system is intended for measuring harmonically related frequency components. Intermods in a narrow band of interest could be evaluated too, but the setup and measurement sequence get more complex as the number of frequencies increases. Kompa [7] proposed a mixed frequency/time domain setup, which is more flexible. However, time base stability and phase tracking errors are not considered. In this paper we will use a time domain approach similar to that of Sipila [8]. The vectorial nonlinear-network analyzer (VNNA), already available for broadband measurements on a fixed equidistant frequency grid [1] is extended for narrowband measurements. An important issue is the calibration of the system, which should now be carried out on a dense grid around the band of interest only. Therefore, we propose a variation of the reference generator absolute calibration method described earlier [1]. The advantages of this new method are a more flexible reference signal, which can easily be adapted for statistically efficient measurements (the covariance matrix of the parameters estimated from the measurements will be minimum). Indeed it was shown that the signal-to-noise ratio during the calibration measurements depends on the crest factor (peak value-to-effective value ratio) of the reference signal. A new method will be described for making narrowband signals with very low crest factors. The uncertainty on the absolute calibration factor will decrease due to this new calibration reference generator.

Once our VNNA is calibrated this way, both amplitude and phase of the Volterra kernels of a narrowband amplifier can be determined accurately. Thanks to the absolute calibration, measurements are repeatable on different VNNA's. The measured kernels can be used to determine the third-order intermodulation and crossmodulation distortion. Also, the accurate knowledge of the Volterra kernels of the main amplifier, both in amplitude and phase, are essential for successful distortion compensation.

II. Reference Signal for Narrowband Calibrations

The absolute calibration of a VNNA requires a reference generator, i.e., a multitone generator with an accurately known output impedance, where the absolute amplitudes and relative phases of all frequency components are stable and accurately specified. This reference generator is characterized by an accurate broadband signal analyzer. A broadband sampling oscilloscope (HP-54121T) is used as a signal analyzer, which means that the calibration is traceable by a nose-to-nose procedure [9]. This method is based on the fact that when the oscilloscope takes a sample, a kick-out pulse is launched to the input connector. This pulse contains information on the scope's characteristic and can be measured with a second oscilloscope. Applying deconvolution techniques, the characteristic of the two scopes can be found, assuming they are identical (this assumption can eventually be avoided by using three oscilloscopes).

The requirements for the reference generator are different for narrowband and broadband measurements. For the narrowband measurements, only frequencies in the band of interest should be present. Also, we will show that a much more flexible signal design is possible now, with higher energy for a given amplitude constraint. This gives lower crest factor signals ($Cr = L_\infty/u_{\text{eff}}$, where L_∞ and u_{eff} are respectively the L-infinity norm or peak value and the effective value of the signal), which results in a higher signal-to-noise ratio during measurement of these signals [10], [11]. For quantization noise

Manuscript received March 7, 1995; revised July 10, 1995. This work was supported by NFWO (Belgian National Fund for Scientific Research) Contract FKFO 2.0034.94.

The author is with Department ELEC, Vrije Universiteit Brussel, B-1050 Brussels, Belgium.

IEEE Log Number 9415452.

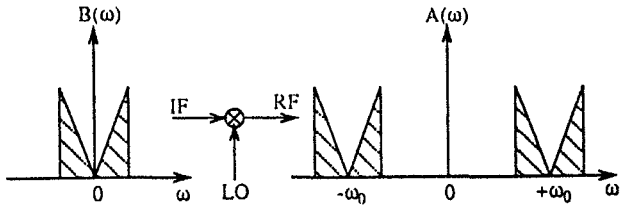

Fig. 1. Spectrum of a double sideband upconverted baseband signal.

we have

$$\frac{S}{N} = 6.02b + 10.8 - 20\log Cr \tag{1}$$

where $(b+1)$ is the number of bits used in the digitalization step.

We will now propose a method for generating narrowband, high-frequency, multisine signals with a low crest factor.

A. Double Sideband Upconversion

Consider an arbitrary bandlimited baseband signal $B(\omega)$. This signal is upconverted to a band around ω_0 using an ideal double sideband mixer to $A(\omega)$ (see Fig. 1)

$$A(\omega) = B(\omega - \omega_0)e^{j\phi} + B(-\omega + \omega_0)e^{-j\phi}. \tag{2}$$

This corresponds to a time domain signal (with $\mathfrak{I}^{-1}$ the inverse Fourier transform)

$$\begin{aligned} a(t, \phi) &= \mathfrak{I}^{-1}[A(\omega)] \\ &= 2b(t)\cos(\omega_0 t + \phi). \end{aligned} \tag{3}$$

Let us now consider the envelope of this time domain signal

$$E_a(t) = \max_\phi [a(t, \phi)] = 2|b(t)| \tag{4}$$

where $b(t)$ is the time domain baseband signal. It can easily be verified that the RMS values are related by

$$\mathrm{RMS}[E_a(t)] = \sqrt{2}\mathrm{RMS}[a(t)]. \tag{5}$$

Since the crest factor is defined as the ratio of peak value-to-effective value

$$\mathrm{Cr}(x) = \frac{x_{\mathrm{peak}}}{x_{\mathrm{rms}}} = \frac{\max_t [|x(t)|]}{x_{\mathrm{rms}}} \tag{6}$$

and since the maximum value of the signal approaches that of the envelope for large $\omega_0/\omega_{\max}$, we have

$$\mathrm{Cr}[a(t)] \leq \sqrt{2}\,\mathrm{Cr}[E_a(t)] = \sqrt{2}\,\mathrm{Cr}[b(t)]. \tag{7}$$

In Fig. 2, an example of an optimized signal is shown. A baseband signal with 12 frequency components of equal amplitude, spaced 1 MHz apart, is considered. This signal is intended for upconversion with a local oscillator of 8013 MHz to a band of 8001–8025 MHz. After optimization, the crest factor of the envelope is 1.39, which means that the complete signal (modulated carrier) will have a crest factor of 1.97.

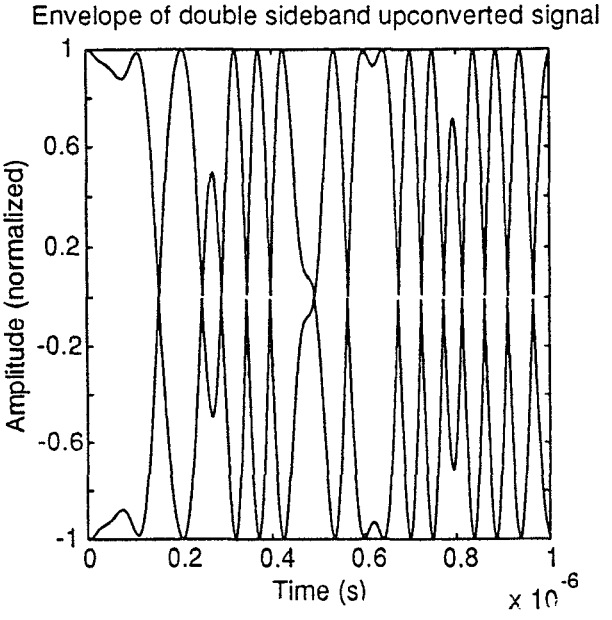

Fig. 2. Envelope $E_a(t)$–double sideband case.

B. Single Sideband Upconversion

Let us now consider the same bandlimited baseband signal $B(\omega) = G(\omega) + G(-\omega)$, this time upconverted to a band around ω_0 using an ideal single sideband mixer (see Fig. 3)

$$A'(\omega) = G(\omega - \omega_0)e^{j\phi} + G(-\omega + \omega_0)e^{-j\phi} \tag{8}$$

where $G(\omega)$ is the one-sided baseband signal (complex).

This corresponds to a time domain signal

$$\begin{aligned} a'(t, \phi) &= \mathfrak{I}^{-1}[A'(\omega)] \\ &= \mathrm{Re}[g(t)e^{j(\omega_0 t + \phi)}]. \end{aligned} \tag{9}$$

The envelope of this time domain signal is

$$E_a(t) = \max_\phi [a'(t, \phi)] = 2|g(t)|. \tag{10}$$

The RMS values of the signal $a'(t)$ and its envelope are related by

$$\mathrm{RMS}[E_{a'}(t)] = \sqrt{2}\,\mathrm{RMS}[a'(t)]. \tag{11}$$

Consequently

$$\mathrm{Cr}[a'(t)] \leq \sqrt{2}\,\mathrm{Cr}[E_{a'}(t)] = \sqrt{2}\,\mathrm{Cr}[g(t)]. \tag{12}$$

This is the same result as for the two-sided case, except that $g(t)$ now is a complex time domain function. Since the crest factor of complex time domain signals can be reduced to lower values (typically, 1.1) than that of real signals (typically, 1.4) [12], the resulting narrowband multisine waveform will also have a lower crest factor.

In Fig. 4, another example of an optimized signal is shown. This time we consider a baseband signal with 25 frequency components of equal amplitude, spaced 1 MHz apart. The frequency band of the upconverted signal is again 8001–8025

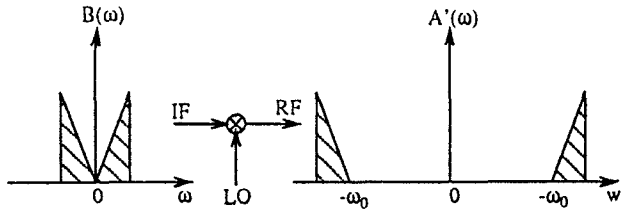

Fig. 3. Spectrum of a single sideband upconverted baseband signal.

MHz. The crest factor of the envelope is now 1.11, and for the complete signal it is 1.58. A zero phase signal with the same amplitude spectrum but with the phases of all components set to zero would have a crest factor of 7.07. According to (1), this means that our single sideband upconverted optimized multisine waveform can be measured with a 13 dB better signal-to-noise ratio than a zero phase signal.

C. Practical Realization of the Reference Generator

The single sideband upconverted multisine described above was realized using an HP 8770A arbitrary waveform synthesizer (26–50 MHz frequency band used) and two mixer stages (LO1 = 800 MHz and LO2 = 7175 MHz) with bandpass filters for selecting the upper sidebands (Fig. 5). This system will be replaced in the future by single sideband mixers. The results of these measurements are shown in Fig. 4. The measured crest factor is 1.85, while the amplitude spectrum is flat within 2 dB in the band of interest. The crest factor is slightly larger than expected due to this 2dB variation and the presence of residual LO and suppressed sidebands (all at least 20 dB down).

III. Narrowband Vectorial Nonlinear -Network Analyzer

A. Measurement Setup

The vectorial nonlinear-network analyzer setup is described in Fig. 7. It consists of a source for generating the test signals, a test set (coupler and power splitter) for isolating the different waves and a data acquisition system (HP54120T sampling oscilloscope). This system is able to coherently measure all harmonics of the incident and scattered waves at the test ports.

Special care has been taken for the synchronization of the source and the data acquisition system. Since we want to measure with a resoltuion of 1 MHz, a trigger signal of 1 MHz has to be generated. It was found that the most stable configuration starts from the 10 MHz reference of the HP83640A sources. After amplification to obtain a steeper voltage transition, the frequency of this signal is divided by 10 (using a circuit based on a SN74LS196N). Finally, the transition time of the 1 MHz signal is reduced with an ultrafast ECL comaprator (AD96685). Using these techniques, together with stable connections in a temperature-controlled room, timing jitter is reduced to 7 ps.

To perform accurate measurements with this network analyzer setup, we need to correct the nonlinearity of the time base of the HP54120T sampling oscilloscope. From the

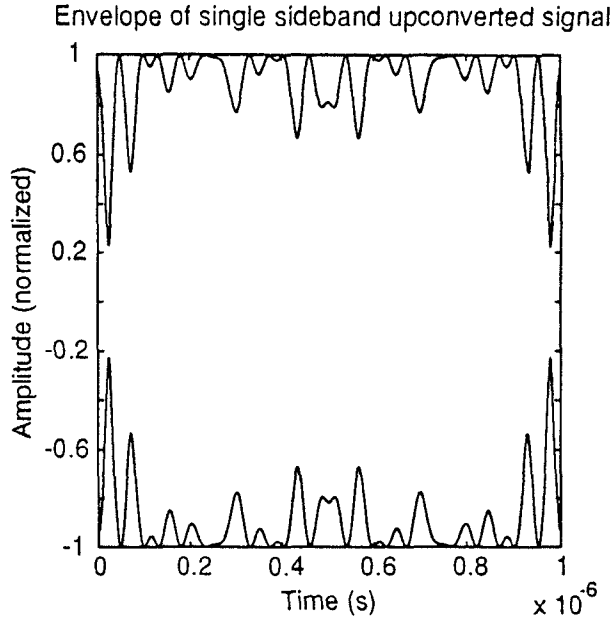

Fig. 4. Envelope $E_a(t)$–single sideband case.

measurement of a time base calibration signal with a known fixed frequency, the time base distortion is determined by mathematical manipulations in the time and frequency domain [13]. The time base distortion, measured over a period of 1 μs (necessary to obtain a frequency resolution of 1 MHz), consists of a linear slope, which varies from one experiment to another, and of a stochastical nonlinear distortion (see Fig. 8). Therefore, we propose a continuous time base calibration (during all experiments) using a signal from the source. According to [13], the frequency of this signal should ideally be around $f_s/4$. In our experiments (sampling frequency f_s = 20.48 GHz), we used the 7.175 GHz signal from within the MMS source and the 8.012 GHz signal from the two-tone source.

To determine the frequency domain data from these measurements on a nonuniform grid, it is not possible to use a classical FFT (for a uniform grid). Therefore, a least-square method was used, in which only the frequency components of interest were estimated. This method was verified with spectrum analyzer amplitude data. Agreement between the sampling oscilloscope and the spectrum analyzer was within 1 dB (without compensation of the time base distortion, deviations up to 15 dB were observed). After time base correction, the dynamic range of our measurment system is 55 dB.

B. Calibration

Define the incoming, reflected and transmitted waves as seen in Fig. 9. Assume that there is a linear relation among the measured waves and the waves at the DUT and that no coupling exists between ports 1 and 2

$$\begin{bmatrix} a_{1d} \\ b_{1d} \\ b_{2d} \end{bmatrix} = \alpha \begin{bmatrix} 1 & e_{12} & 0 \\ e_{21} & e_{22} & 0 \\ 0 & 0 & \gamma \end{bmatrix} \begin{bmatrix} a_{1m} \\ b_{1m} \\ b_{2m} \end{bmatrix} = \alpha[E]\,[C] = \alpha[C_{\text{lin}}]. \tag{13}$$

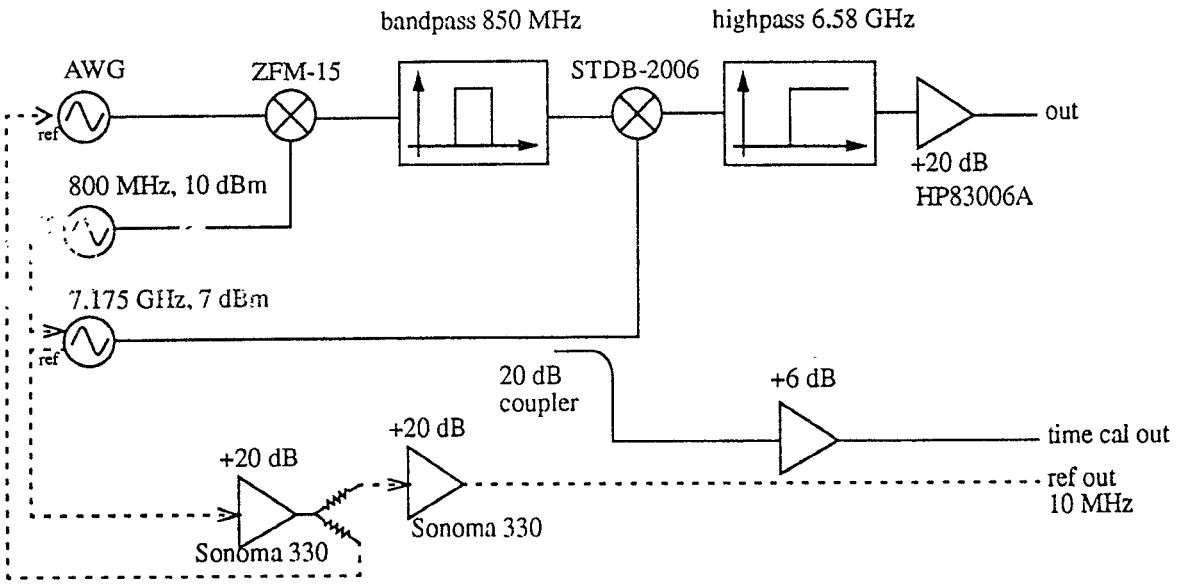

Fig. 5. MMS source.

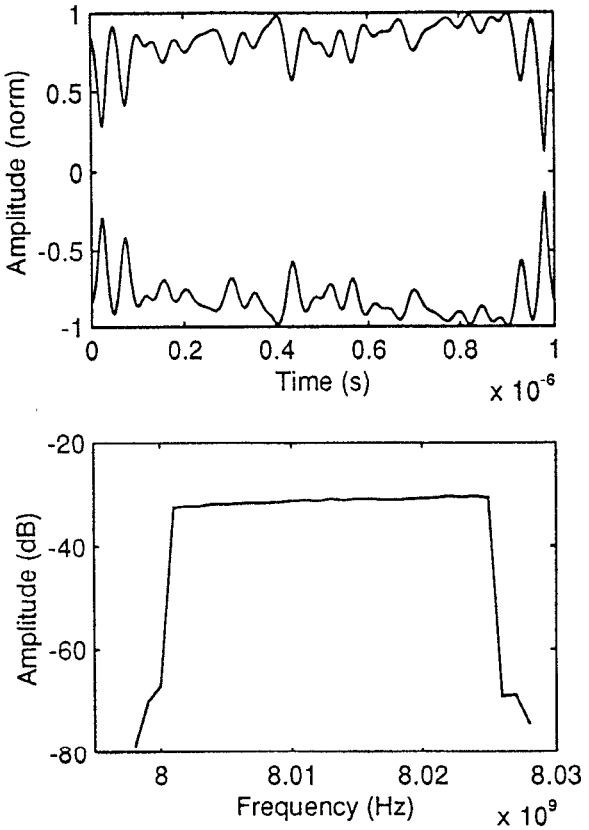

Fig. 6. Measured envelope and amplitude spectrum–single sideband case.

A linear SOLT calibration (short, open, load at port 1 and through) determines $[E]$. The absolute calibration factor α is determined with an absolute calibration using the reference generator [1]

$$\alpha = \frac{b_g}{b'_{d1} - \Gamma_g a'_{d1}} \tag{14}$$

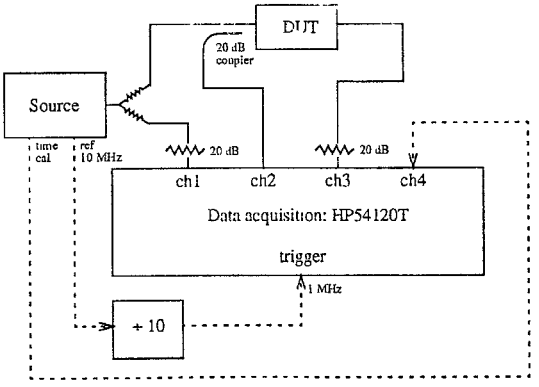

Fig. 7. VNNA setup (overview).

where b_g is the wave emitted by the reference generator, Γ_g the reflection factor of the source, and b'_{d1} and a'_{d1} are the linear calibrated waves at the DUT (from vector $[C_{\text{lin}}]$). In practice, Γ_g has been neglected. The resulting absolute calibration factor α is shown in Fig. 10. Note that the linear part of the phase is arbitrary (the phase of the first frequency has been set to zero). Standard deviations on subsequent measurements of amplitude and phase of α are 0.1 dB and 2 degrees, respectively.

C. Verification

The linear calibration was checked with a 25 Ω airline from an HP8510 verification kit. Good agreement was found (within 0.1 dB and 5°) for the band of interest (8.001–8.025 GHz). The absolute calibration was verified with a power meter calibration for the amplitude of α. Agreement within 0.5 dB was found. The phase of α was not verified since no absolute phase verification technique exists. Eventually, the validity of the absolute phase calibration could have been checked with a method similar to that described in [1].

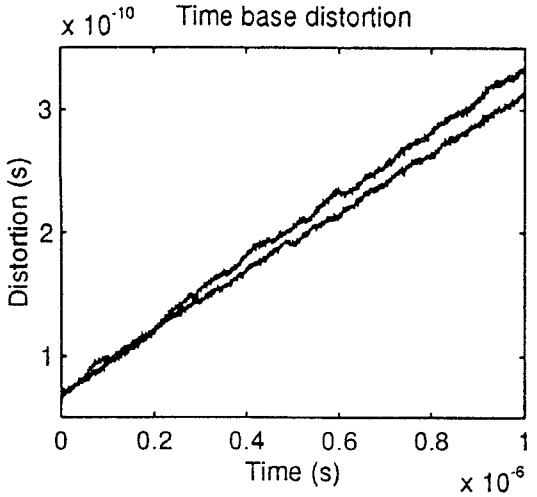

Fig. 8. Time base distortion of two subsequent measurements.

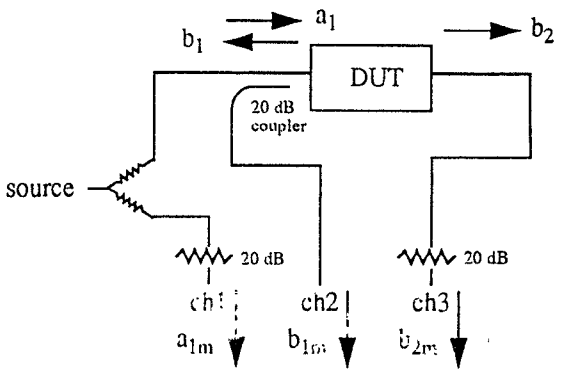

Fig. 9. Definition of waves.

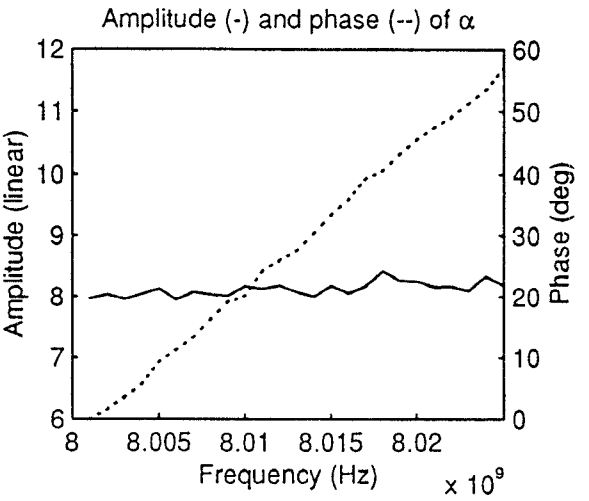

Fig. 10. Absolute calibration factor α.

IV. Intermodulation and Crossmodulation

A. Volterra Formulation

Start from a general Volterra formulation for weakly nonlinear systems [3], with input at port 1 and output at port 2

$$b_2(n) = \sum_{i=1}^{\infty} \frac{i!}{m_{1i}! \cdots m_{si}!} \sum_{k_1+\cdots+k_i=n} a_1(k_1) \cdots a_1(k_i) \cdot H_i(k_1, \cdots, k_i) \quad (15)$$

(output b_2 at frequency nf_0, input a_1 at frequencies kf_0 with multiplicity m for each i-th order Volterra kernal H_i). We suppose that only the linear terms and the third-order nonlinearities are important (second order are out of band, higher order neglected). If the input contains the frequencies ω_1 and ω_2, then the output at $2\omega_2 - \omega_1$ can be written as

$$b_2[j(2\omega_2 - \omega_1)] = \frac{3!}{2!1!} a_1(-j\omega_1)a_1(j\omega_2)a_1(j\omega_2) \cdot H_3(-j\omega_1, j\omega_2, j\omega_2). \quad (16)$$

At ω_1

$$\begin{aligned} b_2(j\omega_1) = {} & a_1(j\omega_1)H_1(j\omega_1) \\ & + \frac{3!}{2!1!} a_1(-j\omega_1)a_1(j\omega_1)a_1(j\omega_1) \\ & \cdot H_3(-j\omega_1, j\omega_1, j\omega_1) \\ & + \frac{3!}{1!1!1!} a_1(-j\omega_2)a_1(j\omega_1)a_1(j\omega_2) \\ & \cdot H_3(-j\omega_2, j\omega_1, j\omega_2). \end{aligned} \quad (17)$$

Since we assume small nonlinearities, the third-order terms in (17) will be neglected.

B. Intermodulation and Crossmodulation from Volterra Kernels

If the input consists of two frequencies ω_1 and ω_2 of equal amplitude, intermodualtion IM_3 is defined as the amplitude of the ratio of the distortion product to the fundamental signal in the output

$$IM_3 = \left| \frac{b_2(j(2\omega_2 - \omega_1))}{b_2(j\omega_2)} \right| = 3 \left| \frac{a_1^*(j\omega_1)a_1(j\omega_2)a_1(j\omega_2)}{a_1(j\omega_1)} \frac{H_3(-j\omega_1, j\omega_2, j\omega_2)}{H_1(j\omega_1)} \right|. \quad (18)$$

If we specify the input as

$$a_1 = \left[\frac{A_c}{2} e^{j\alpha} \delta(\omega - \omega_1) + \frac{A_c}{2} e^{j\beta} \delta(\omega - \omega_2) \right] + CC \quad (19)$$

where CC stands for the complex conjugate of the first term, (18) reduces to

$$IM_3 = \frac{3}{4} \left| A_c^2 e^{j2(\beta-\alpha)} \frac{H_3(-j\omega_1, j\omega_2, j\omega_2)}{H_1(j\omega_1)} \right| = \frac{3}{4} A_c^2 \left| \frac{H_3(-j\omega_1, j\omega_2, j\omega_2)}{H_1(j\omega_1)} \right|. \quad (20)$$

Frequency domain crossmodulation CM_F for two frequencies ω_1 and ω_2, where the first is amplitude modulated with ω_m, is defined as the amplitude of the ratio of the transferred fractional modulation to the original fractional modulation, measured in the output. Therefore, the values of the following

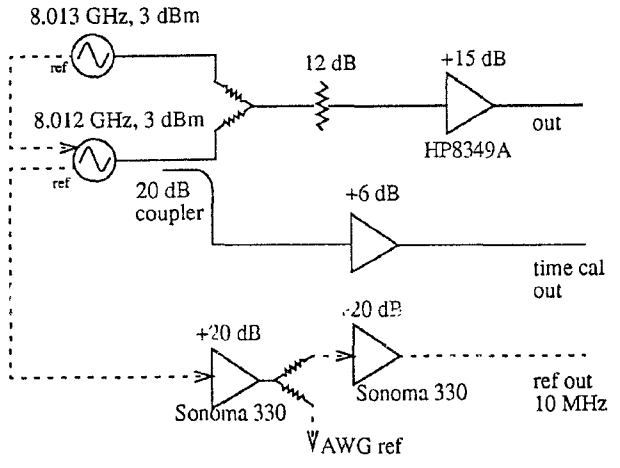

Fig. 11. Two-tone source.

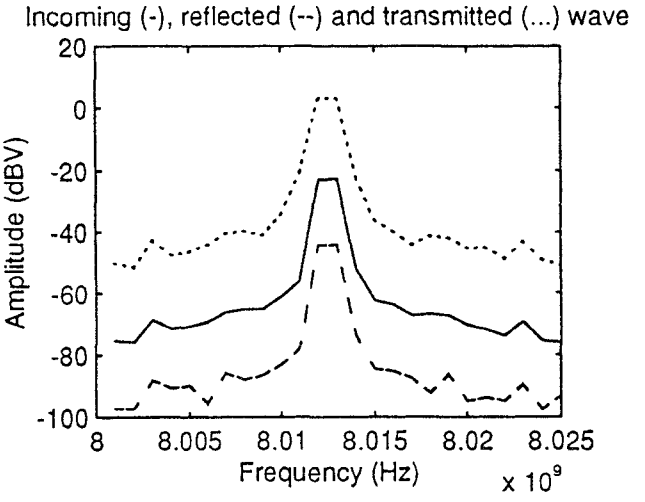

Fig. 12. Incoming and scattered waves of the intermodulation experiment.

waves must be found

$$
\begin{aligned}
b_2(j\omega_1) &= a_1(j\omega_1)H_1(j\omega_1) + \cdots \\
b_2[j(\omega_1+\omega_m)] &= a_1[j(\omega_1+\omega_m)]H_1[j(\omega_1+\omega_m)] + \cdots \\
b_2(j\omega_2) &= a_1(j\omega_2)H_1(j\omega_2) + \cdots \\
b_2[j(\omega_2+\omega_m)] & \\
&= \frac{3!}{1!1!1!}\, a_1[-j(\omega_1-\omega_m)]a_1(j\omega_1)a_1(j\omega_2) \\
&\quad \cdot H_3[-j(\omega_1-\omega_m),\, j\omega_1,\, j\omega_2] \\
&\quad + \frac{3!}{1!1!1!}\, a_1(-j\omega_1)a_1[j(\omega_1+\omega_m)]a_1(j\omega_2) \\
&\quad \cdot H_3[-j\omega_1,\, j(\omega_1+\omega_m),\, j\omega_2] \\
&\cong 6H_3(-j\omega_1,\, j\omega_1,\, j\omega_2)a_1(j\omega_2)\{a_1(j\omega_1) \\
&\quad \cdot a_1^*[j(\omega_1-\omega_m)] + a_1^*(j\omega_1)a_1[j(\omega_1+\omega_m)]\}
\end{aligned}
\tag{21}
$$

(again neglecting higher-order terms at ω_1, ω_2 and $\omega_1+\omega_m$). The crossmodulation now equals

$$
CM_F = \left| \frac{b_2(j(\omega_2+\omega_m))/(b_2(j\omega_2))}{b_2(j(\omega_1+\omega_m))/(b_2(j\omega_1))} \right|. \tag{22}
$$

If the input is more explicitly written as (noting one carrier is amplitude modulated)

$$
\begin{aligned}
a_1 &= \frac{A_c}{2}\, e^{j\alpha}\delta(\omega-\omega_1) + \frac{A_c}{2} e^{j\beta}\delta(\omega-\omega_2) \\
&\quad + \frac{A_c m}{4}\, e^{j(\alpha-\gamma)}\delta(\omega-(\omega_1-\omega_m)) \\
&\quad + \frac{A_c m}{4}\, e^{j(\alpha+\gamma)}\delta(\omega-(\omega_1+\omega_m)) + CC
\end{aligned}
\tag{23}
$$

(where CC is the complex conjugate on the negative frequency axis), we find the crossmodulation

$$
CM_F = 3A_c^2 \left| \frac{H_3(-j\omega_1,\, j\omega_1,\, j\omega_2)}{H_1(j\omega_1)} \right|. \tag{24}
$$

If ω_1 and ω_2 are close together, then $CM_F \cong 4IM_3$ (cf. [14]). Define

$$
\phi = \angle H_3(-j\omega_1,\, j\omega_1,\, j\omega_2) - \angle H_1(j\omega_1). \tag{25}
$$

TABLE I
VOLTERRA KERNELS

	Amplitude	Phase (deg)
H1	19.9	143.1
H3	39.6V^{-2}	10.1

TABLE II
IM EXPERIMENT

	IM$_3$ (dB)	phase (deg)
VNNA	-25.6	-133.0
SA	-26.6	-

Equation (24) can be split into amplitude crossmodulation, $CM_F \cos\phi$, and phase crossmodulation, $CM_F \sin\phi$ [15]. Notice that this can be done only if calibrated amplitude and phase measurements of the Volterra kernels are available.

C. Practical Results

Using the VNNA setup, the nonlinearities in an HP83006A amplifier were measured. As a test signal, the two-tone source described in Fig. 11 was used. The resulting calibrated waves are shown in Fig. 12. From these results, some of the Volterra kernels of the system can be determined (assuming a weakly nonlinear system, i.e., only linear and third-order terms are considered; third-order terms are neglected if the linear term is present). See Table I.

The results of this intermodulation experiment were compared with spectrum analyzer (SA) measurements (see Fig. 13 and Table II).

Note that the VNNA measurements also give the phase of IM_3. From this intermodulation experiment, the crossmodulation can be determined using the Volterra kernel formulation (small distortion). These results were compared with spectrum analyzer data from a crossmodulation experiment (see Fig. 14 and Table III).

TABLE III
CM EXPERIMENT

	CM_F (dB)	CM_A(dB)	CM_P(dB)	ϕ (deg)
VNNA	-13.6	-16.2	-16.9	-133.0
SA	-13.3	-	-	-

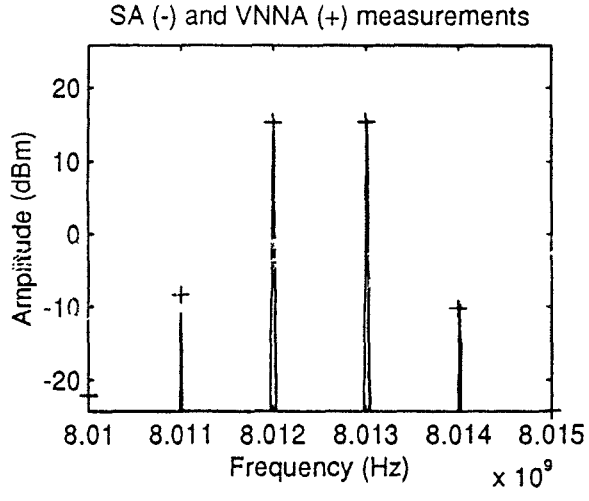

Fig. 13. Output spectrum of the intermodulation experiment (input: −5 dBm at 8.012 GHz and −5 dBm at 8.013 GHz).

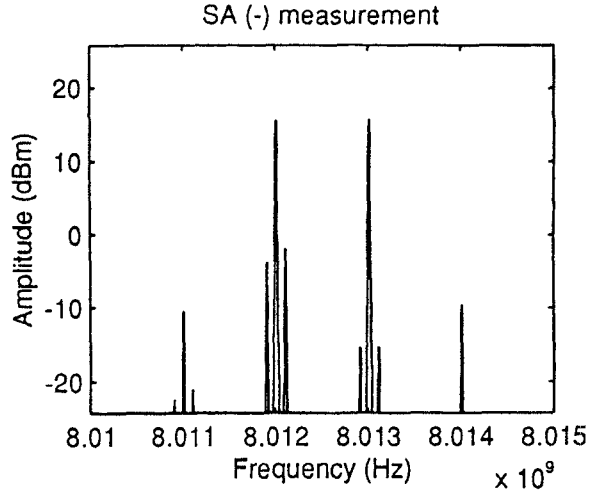

Fig. 14. Output spectrum of the crossmodulation experiment (input: −5 dBm at 8.012 GHz, 50% AM modulated).

Where the amplitudes are concerned, the VNNA and SA measurements agree within 1 dB; however, the VNNA measurements give extra phase information facilitating differentiation between amplitude crossmodulation CM_A (AM to AM) and phase crossmodulation CM_P (AM to PM).

V. Feedforward Amplifier Compensation

The feedforward amplifier of Fig. 15 consists of a nonlinear main amplifier G (with a linear part G_1 and a third-order part G_3), a linear error amplifier A_2, networks T_1 and T_2 (delay τ_1 and τ_2, respectively, plus a small frequency independent amplitude correction), couplers and dividers with coupling coefficients k_i and $\tilde{k}_i$. Assume that the amplifiers are unilateral and that the amplifiers and delay networks are matched at their inputs. The overall amplifier can now be described by its first- and third-order Volterra kernels [15]

$$H_1(j\omega) = k_1 a_1 e^{-j\omega\tau_1} k_4 A_2(j\omega) k_3 + \tilde{k}_1 G_1(j\omega)[\tilde{k}_2 a_2 e^{-j\omega\tau_2}\tilde{k}_3 - k_2\tilde{k}_4 A_2(j\omega)k_3] \quad (26)$$

$$H_3(j\omega_1, j\omega_2, j\omega_3) = \tilde{k}_1^3 G_3(j\omega_1, j\omega_2, j\omega_3) \cdot [\tilde{k}_2 a_2 e^{-j(\omega_1+\omega_2+\omega_3)\tau_2}\tilde{k}_3 - k_2\tilde{k}_4 A_2(j\omega_1 + j\omega_2 + j\omega_3)k_3]. \quad (27)$$

From (20), (24), and (27) it follows that intermodulation and crossmodulation can be made zero if

$$|A_2(\omega)| = \frac{\tilde{k}_2\tilde{k}_3 a_2}{k_2\tilde{k}_4 k_3}$$
$$\angle A_2(\omega) = -\omega\tau_2 \quad (28)$$

at $\omega = 2\omega_2 - \omega_1$ for intermodulation and at $\omega = \omega_2$ for crossmodulation. However, if a small amplitude imbalance δa and a phase imbalance $\delta\phi$ remain in the second loop

$$\delta a = \frac{k_2\tilde{k}_4 k_3}{\tilde{k}_2\tilde{k}_3 a_2}|A_2|$$
$$\delta\phi = -\angle A_2 - \omega\tau_2 \quad (29)$$

a residual intermodulation and crossmodulation remain [15]

$$\gamma = \frac{IM_{3FF}}{IM_3} = \sqrt{(1-\delta a)^2 + (\delta a\delta\phi)^2}$$
$$\psi = \phi_{FF} - \phi = \operatorname{atan}\frac{\delta a\delta\phi}{1-\delta a} \quad (30)$$

(no index: main amplifier without feedforward; FF: feedforward amplifier with imbalance). The values of γ and ψ can be measured with a VNNA. By solving (30), the amplitude imbalance δa and phase imbalance $\delta\phi$ can be found

$$\delta a = 1 - \sqrt{\frac{\gamma^2}{1+(\tan\psi)^2}}$$
$$\delta\phi = \frac{1-\delta a}{\delta a}\tan\psi. \quad (31)$$

This enables a further compensation of the distortion of the feedforward amplifier. Note that both amplitude and phase measurements of IM_3 and CM_F are necessary, which is possible with a calibrated VNNA.

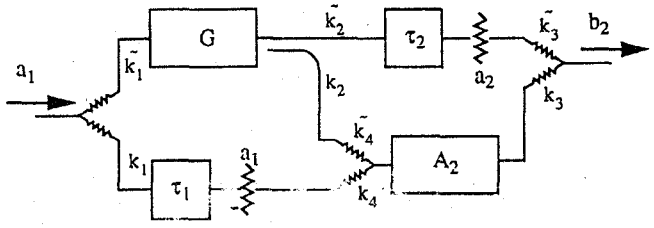

Fig. 15. Feedforward amplifier.

VI. Conclusion

The use of a vectorial nonlinear-network analyzer in narrowband applications has been demonstrated. The need for an accurate absolute calibration requires a new technique based on a narrowband reference generator with a low crest factor to allow a calibration with a high statistical efficiency. A method for realizing such a signal is described based on upconverting a baseband signal and a new crest factor optimization technique. The calibrated VNNA is then used to measure the Volterra kernels of a narrowband amplifier. These results can be used to compensate for the intermodulation and crossmodulation in a feedback or feedforward amplifier configuration.

References

[1] T. Van den Broeck and J. Verspecht, "Calibrated vectorial nonlinear-network analyzers," in *IEEE MTT-S Int. Microwave Symp. Dig.*, San Diego, 1994, pp. 1069–1072.

[2] F. Verbeyst and M. Vanden Bossche, "Viomap, the S-parameter equivalent for weakly nonlinear rf and microwave devices," in *IEEE MTT-S Int. Microwave Symp. Dig.*, San Diego, 1994, pp. 1369–1372.

[3] M. Vanden Bossche, "Measuring nonlinear systems: A black box approach for instrument implementation," Ph.D. dissertation, Vrije Universiteit Brussel, May 1990.

[4] S. A. Maas, "Modeling the gate I/V characteristic of a GaAs MESFET for Volterra-series analysis," *IEEE Trans. Microwave Theory Tech.*, vol. 37, pp. 1134–1136, July 1989.

[5] ——, *Nonlinear Microwave Circuits.* Norwood, MA: Artech House, 1988.

[6] U. Lott, "Measurement of magnitude and phase of harmonics generated in nonlinear microwave two-ports," *IEEE Trans. Microwave Theory Tech.*, vol. 37, pp. 1506–1511, Oct. 1989.

[7] G. Kompa and F. Van Raay, "Error-corrected large-signal waveform measurement system combining network analyser and sampling oscilloscope capabilities," *IEEE Trans. Microwave Theory Tech.*, vol. 38, pp. 358–365, Apr. 1990.

[8] M. Sipila, K. Lehtinen, and V. Porra, "High-frequency periodic time-domain waveform measurement system," *IEEE Trans. Microwave Theory Tech.*, vol. 36, pp. 1397–1405, Oct. 1988.

[9] J. Verspecht and K. Rush, "Individual charactrization of broadband sampling oscilloscopes with a nose-to-nose calibration procedure," *IEEE Trans. Instrum. Meas.*, vol. 43, pp. 347–354, Apr. 1994.

[10] J. Schoukens and R. Pintelon, *Identification of Linear Systems.* Oxford: Pergamon, 1991.

[11] T. Van den Broeck, R. Pintelon, and A. Barel, "Design of a microwave multisine source using allpass functions estimated in the richards domain," *IEEE Trans. Instrum. Meas.*, vol. 43, pp. 753–757, Oct. 1994.

[12] J. Schoukens, Y. Rolain, and P. Guillaume, "Design of narrow band, high resolution multisines," ELEC internal report, JS3/94.

[13] J. Verspecht, "Accurate spectral estimation based on measurements with a distorted-timebase digitizer," *IEEE Trans. Instrum. Meas.*, vol. 43, pp. 210–215, Apr. 1994.

[14] R. G. Meyer, M. J. Shensa, and R. Eschenbach, "Cross modulation and intermodulation in amplifiers at high frequencies," *IEEE J. Solid-State Circuits*, vol. 7, pp. 16–23, Feb. 1972.

[15] A. Javed, P. A. Goud, and B. A. Syrett, "Analysis of microwave feedforward amplifier using Volterra series representation," *IEEE Trans. Commun.*, pp. 355–360, Mar. 1977.

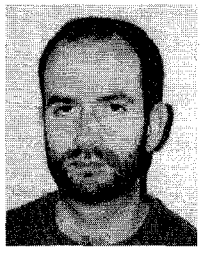

Tom Van den Broeck was born in Deurne, Belgium, January 15, 1965. He received the engineer and the Ph.D. degrees from the University of Brussels (VUB) in 1988 and 1995, respectively.

He is presently a Research Assistant at the Department of Fundamental Electricity and Instrumentation (ELEC) at the University of Brussels. His current research is in the field of microwave measurements, calibration, and parameter estimation.